Journal of Nano- and Electronic Physics
Vol. **16** No 6, 06013(6pp) (2024)

Журнал нано- та електронної фізики
Том **16** № 6, 06013(6cc) (2024)

REGULAR ARTICLE

Application of Bifacial Solar Cells on Cadmium Telluride Base to Determine the Wavelength of Pulsed Laser Diode Radiation

G.S. Khrypunov[1,2,*], A.I. Dobrozhan[1], M.V. Kirichenko[1], R.V. Zaitsev[1], M.S. Khrypunov[1], A.V. Meriuts[1]

[1] *National Technical University «Kharkiv Polytechnic Institute», 61002 Kharkiv, Ukraine*
[2] *Ecole Polytechnique Fédérale de Lausanne, CH-1015 Lausanne, Switzerland*

(Received 20 September 2024; revised manuscript received 10 December 2024; published online 23 December 2024)

A physical concept of the simple, economical, and compact method for determining the wavelength of pulsed laser diode radiation has been proposed. In this method, the bifacial thin film solar cell (SC) SnO_x:F/CdS/CdTe/ITO is used as a sensor that detects the wavelength of incident pulsed radiation. When implementing the method, SnO_x:F/CdS/CdTe/ITO solar cell is illuminated from the back and front sides by pulsed radiation of the laser diode. Constant direct voltage biases in the 0-1.2 V range are applied to the solar cell when illuminated from the front side. When illuminating the solar cell from the back side, along with a similar direct voltage bias, reverse voltage biases in the 0-1.5 V range are applied. The wavelength is determined by comparing, with the help of a computer program, the obtained values of the short-circuit current, which is generated during the irradiation of the SC, with the previously obtained numerical database of the spectral dependence of the short-circuit current of the given SC.

Keywords: Bifacial solar cells, Cadmium telluride, Wavelength, Pulsed laser diode, Quantum efficiency coefficient, Voltage bias.

DOI: 10.21272/jnep.16(6).06013 PACS numbers: 07.60.Rd, 85.60. – q

1. INTRODUCTION

Laser diodes are widely used electronic components [1]. They are used as controlled light sources in optical fiber communication lines and various measuring equipment, such as laser rangefinders. Another common application is barcode reading. Laser diodes with visible radiation, usually red and sometimes green, are used in crosshairs. Infrared and red lasers are used in CD and DVD players. Blue lasers are used in HD DVD and Blu-Ray devices. There are many situations when it is necessary to measure the wavelength of laser diodes: at the stage of industrial production to carry out their initial control, if it is necessary to precisely adjust the radiation of laser diodes to a particular wavelength, to analyze the degradation associated with the conditions or period of operation, and others. Therefore, improving existing and developing new methods of measuring the length of electromagnetic waves and the devices that implement them remains an urgent physical and technical task. At the same time, not only the accuracy of wavelength measurement but also the speed of the implemented technique, the compactness, and the economy of the device that implements this technique. All modern devices for measuring wavelength work based on the spatial distribution of radiation with different wavelengths using interference or diffraction. At the same time, the diffraction or interference picture of the investigated radiation is compared with the standard [2]. In recent years, computerized analyzers with sensors based on lines of photodiodes, which are linear image sensors, have been developed to determine the wavelength [3]. The principle of operation is that the radiation whose wavelength must be determined is sent to the diffraction grating, which is used to spread the radiation spatially. Expanded radiation enters the focal plane with a linear image sensor of 2043-4096 photodiodes. Each photodiode, which is a pixel, shows its part of the spectrum. Analog signals proportional to the intensity of the incident radiation and the accumulation time from the outputs of the discrete photodiodes are sent to the analog-to-digital converter. They are then digitally sent to the control computer. Before starting work, the device is calibrated. For this, the spectra of a mercury or neon lamp are recorded, and the position of the spectral lines and the ratio of their intensity are well-known.

There is another physical possibility of spatial separation of radiation with different wavelengths. Thus, the light absorption depth in implementing the internal photo effect in semiconductors decreases exponentially with increasing wavelength. However, the use of this physical effect to determine the wavelength in traditional solar cells (SCs) based on crystalline silicon is hindered by the fact that, due to the illumination of the device structure from the side of the space charge region (SCR) and low volume recombination, the contribution to the photocurrent from non-equilibrium charge carriers generated under the action of radiation from different wavelengths and

* Correspondence e-mail: khrip@ukr.net

Cite this article as: G.S. Khrypunov et al., *J. Nano- Electron. Phys.* 16 No 6, 06013 (2024) https://doi.org/10.21272/jnep.16(6).06013

do not differ significantly. A different situation is realized in the bifacial thin film solar cells based on cadmium telluride developed by us [4]. A transparent ITO electrode was used as the rear contact in such an SC, which spatially separates the region of active generation of non-equilibrium carriers from the area of the built-in electric field. A CdTe/ITO tunnel rear contact with a height of 2.2 eV is an additional physical factor that distinguishes the developed bifacial sensitive SC [5].

Therefore, we have introduced the study of the spectral dependence of the photo-response to create a method of using bilaterally sensitive solar cells based on cadmium telluride to determine the wavelength of pulsed laser diodes.

2. EXPERIMENTAL

The method of determining the wavelength of pulsed laser diode radiation is using bifacial SnO_x:F/CdS/CdTe/ITO thin film SCs. For the manufacture of laboratory samples, a CdTe/CdS heterosystem was formed by the method of sequential low-temperature (< 450 °C) thermal vacuum evaporation of layers of cadmium sulfide with a thickness of 0.4 μm and cadmium telluride with a thickness of 4 μm on glass plates coated with SnO_x:F, with a thickness of 2 mm. After the structure was obtained, chloride treatment was carried out to increase the photosensitivity of the base layer of cadmium telluride and optimize the properties of the back separating barrier at the CdTe/CdS interface [6]. Then, to remove the products of chemical reactions that occurred during the chloride treatment and obtain a layer of tellurium to form the tunnel back contact, the surface of cadmium telluride was etched in a solution of bromine in methanol. Then, a transparent and electrically conductive film layer of indium tin oxide (ITO) was obtained to the etched surface of the base layer by magnetron sputtering to create back contact with the cadmium telluride layers. Thin metal contacts were deposited on the ITO surface. The unique feature of the solar cell is the presence of transparent back and front contacts. Therefore, the solar element can be lit both from the front and the back (Fig. 1). The active area of a separate SC, which was separated by scribing, was 0.5 cm^2 (Fig. 1, b)

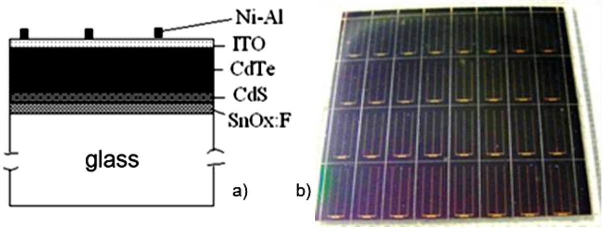

Fig. 1 – Laboratory sample of SC SnO_x:F/CdS/CdTe/ITO a – a diagram of the instrument structure, b – a SC photo

We conducted studies of the spectral dependence of the external quantum efficiency coefficient $Q(\lambda)$, which allows us to determine the efficiency of photovoltaic processes depending on the incident radiation wavelength. The quantum efficiency coefficient Q is the ratio of the number of charge carriers contributing to the photocurrent to the total number of photons arriving at the SC active surface. There is a functional relationship between the short-circuit photocurrent and the quantity $Q(\lambda)$, which is described for a sufficiently large SC shunt resistance by the ratio [7]:

$$Q(\lambda) = (J_{ph}/I)(hc)/(e\lambda) \quad (1)$$

where $J_{\rm ph}$ is the short-circuit photocurrent density generated under monochromatic light illumination, λ and I are, respectively, the wavelength and intensity of the monochromatic light, e is the elementary charge, h is the plank constant, c is the speed of light in vacuum.

The spectral dependence of the short-circuit current of the SC was measured using a special optical-electric circuit, the photo of which is shown in Figure 2.

The system consists of a Ge2144-01 halogen lamp with Power Supply SM 300-5 power supply units and Lampenhaus TYP LAX 1000 cooling (Fig. 3, 1), a light pulse modulator Beam Chopper 230 (Fig. 3, 6), a diffraction monochromator (Fig. 3, 10) and the Transimpedanzverstaerkep FHG-ISE detector unit (Fig. 3, 3).

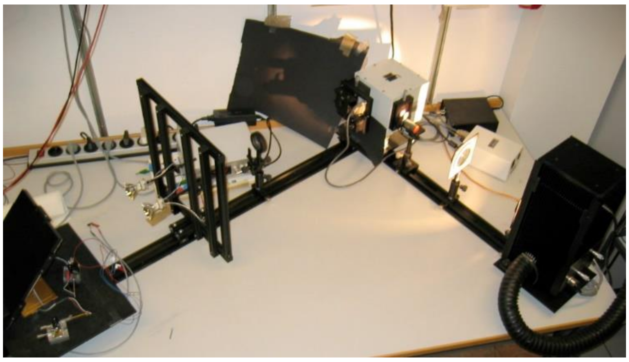

Fig. 2 – Photograph of an optical-electronic circuit for measuring the spectral dependence of the short-circuit current

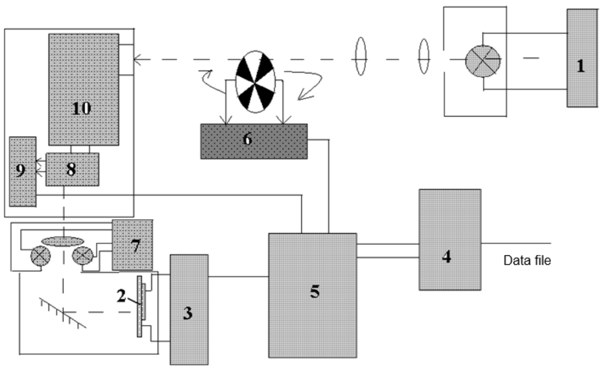

Fig. 3 – Block diagram of the optical-electrical system for measurement spectral dependences of the short-circuit current

The detector unit is designed to estimate the amplitude of photocurrent oscillations generated by the solar cell (Fig. 3, 2) when illuminated by a pulsed light signal. Measurement management and electrical signal processing are carried out using a personal computer connected to the rest of the blocks by a special collector (Fig. 3, 5), according to the LabViewTM5.1 program (Fig. 3, 4). The SC samples under test are placed in a shaded enclosure for measurements. The necessary dimensions of the light beam are set with the help of special membranes depending on the active area of the SC under investigation (Fig. 3, 7). Before taking measurements, the radiation spectrum is warmed up for an hour to stabilize it. Then, calibration of the intensity of the radiation incident on the sample is carried out according to the reference spectral dependences of the absolute values of the quantum efficiency of the test silicon SC with a step of 5-20 nm. A program that regulates the wavelength of the light signal applied to the solar cell controls the monochromator using a personal computer. For this, the optical window (Fig. 3, 8) is automatically shifted along the spectrum generated by the diffraction grating (Fig. 3, 9). As a result, each position of the window corresponds to a particular wavelength of the light signal in the range from 0.365 µm to 1.189 µm. To avoid the influence of external light sources on the measurement results, the light flux was modulated with a frequency of 230 Hz. This makes it possible to compensate for the constant component of the SC photocurrent during measurements (Fig. 3, 3-6) and increase the accuracy of measurements. In addition, it makes it possible to study the influence of the constant voltage applied to the SC on the efficiency of photovoltaic processes [8]. During processing, the amplitude of the generated SC electric signal was compared with the data for the reference SC obtained during calibration, which allows for calculating both the relative and absolute values of $Q(\lambda)$ for each wavelength of the incident radiation.

3. RESULTS AND DISCUSSION

The spectral dependences of $Q(\lambda, U)$ CdS/CdTe/ITO SC under illumination from the frontal side and direct voltage displacement were investigated (Fig. 4)

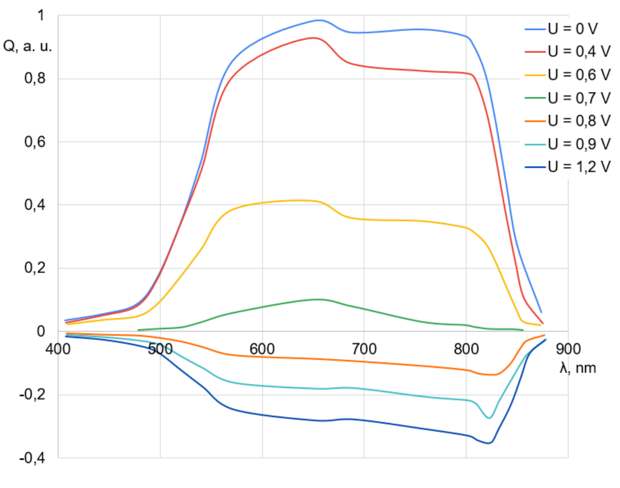

Fig. 4 – The effect of direct voltage bias on $Q(\lambda, U)$ of SnO_x:F/CdS/CdTe/ITO SC when illuminated from the front side

We used the well-known theoretical provisions fully outlined in [8] to analyze the obtained results. According to these provisions, the value of the quantum efficiency coefficient $Q(\lambda, U)$ of a single-pass SC is determined by the theoretical expression:

$$Q(\lambda, U) = G(\lambda)H(\lambda, U), \quad (2)$$

where $G(\lambda)$ is the generation efficiency, which is the ratio of the number of generated electron-hole pairs to the number of photons arriving at the SC surface; $H(\lambda, U)$ is the collection coefficient, which depends on the applied voltage and is the ratio of the number of generated electron-hole pairs to the charge carriers that contribute to the creation of the photocurrent.

The value of SC's $G(\lambda)$is determined by the amount of optical losses and the spectral dependence of the light absorption depth in the base layer. The value SC's $H(\lambda, U)$ is determined by volume and surface recombination in the base layer:

$$H(\lambda, U) = h_v(\lambda, U)h_s(U), \quad (3)$$

where $h_v(\lambda, U)$ is the coefficient U of loss of non-equilibrium charge carriers as a result of their volume recombination in the area of the base layer outside the space charge area (SCA) of the separating barrier; $h_s(U)$ is the coefficient of loss of non-equilibrium charge carriers inside the SCA.

At the same time, $h_v(\lambda, U)$ is determined by the expression:

$$h_v(\lambda, U) = (1 - \exp[- w(U)/l(\lambda)])/[1 + L_n/l(\lambda)], \quad (4)$$

where $w(U)$ is the thickness of the SCA separating barrier; $l(\lambda)$ is the photon absorption depth; L_n is the diffusion length of an electron in the base layer of cadmium telluride.

According to theoretical provisions, recombination in the area of the space charge of the separating barrier can be described as surface recombination:

$$h_s(U) = 1/[1 + S/(\mu E)], \quad (5)$$

where S is the speed of surface recombination; μ is the mobility of electrons in the base layer; E is the intensity of the built-in electric field inside the depletion region.

At the same time, the value of E is determined by the expression:

$$E = 2(\varphi_d - U)/w(U) \quad (6)$$

where φ_d is the height of the separating barrier.

In the final stage of photoelectric conversion of solar energy – the collection of non-equilibrium charge carriers generated under the action of light by the back and front electrodes- there are losses due to the electrical resistance of real electrical contacts to p and n areas of the device structure. According to [9], the physical mechanisms described above describe experimental $Q(\lambda, U)$ CdS/CdTe SCs with conventional back electrodes. To apply a similar approach to the analysis of photovoltaic conversion in ITO/CdTe/CdS SC, it is necessary to take into account that with a direct bias, the n^+-ITO/p^+-CdTe tunnel contact can form a region of the built-in electric field [5].

According to the obtained experimental data, when illuminated from the frontal side and the direct displacement of the applied voltage increases, it decreases the entire spectral range of photosensitivity (Fig. 4). According to expression (6), the increase in positive displacement voltage leads to a decrease in the intensity of the built-in electric field in the space charge area. This causes an increase in losses of non-equilibrium charge carriers in the space charge area (5). According to (5), the loss amount does not depend on the radiation wavelength. An increase in the positive displacement also leads to a decrease in the thickness of the space charge region, which, accordingly, causes an increase in the recombination losses of charge carriers in the volume (4). These losses increase with increasing wavelength by the increase in the depth of light absorption, which removes the region of active generation of non-equilibrium charge carriers from the SCA. Thus, the change in $Q(\lambda, U)$ with increased direct displacement is due to the joint action of both described physical mechanisms. According to the existing theoretical ideas, when the direct displacement increases above the height of the potential barrier, the thickness of the SCA decreases to zero, and the separation of non-equilibrium charge carriers stops. As a result, $Q(\lambda, U)$ becomes zero in the entire spectral range of photosensitivity. However, for the studied SnO_x:F/CdS/CdTe/ITO SCs, depending on $Q(\lambda, U)$ and the value of the forward bias, a change in the polarity of the photocurrent from positive to negative is observed. At the same time, the amount of voltage corresponding to the change in polarity decreases with the increase in the wavelength of the incident radiation. At $U \sim 0.8$ V, the photocurrent's polarity change occurs in the entire spectral range of photosensitivity of the device structure. Figure 4 presents this circumstance's dependencies – $Q(\lambda, U)$. In [10], for *n*-CdS/*p*CdTe/Sb_2Te_3 SC with a direct shift in the narrow spectral range (820-900) nm also observed a change in the polarity of the photocurrent. According to the authors of this work, the increase in direct elimination leads to an increase in the thickness of the space charge region of the back tunnel contact *p*CdTe/Sb_2Te_3. Indeed, the direct elimination of the *n*-CdS/*p*CdTe front heterojunction is reversed for the *p*-CdTe/Sb_2Te_3 back contact. Therefore, with a sufficiently large direct displacement, the separation of charge carriers is carried out in the space charge formed at the back contact boundary. This leads to the generation of a photocurrent in the direction opposite to the original one. In our opinion, in SnO_x:F/CdS/CdTe/ITO SC, the change in the polarity of the photocurrent is due to the existence of two heterojunctions (HJs) connected one to the other: *n*-CdS-*p*CdTe and p^+-CdTe-n^+-ITO. When the forward bias increases, the electrical resistance of *n*-CdS-*p*-CdTe decreases, and a significant part of the applied voltage falls on the p^+-CdTe-n^+-ITO HJ, for which this voltage polarity creates a reverse bias. Therefore, the SCA of the p^+-CdTe-n^+-ITO HJ begins to grow, which leads to the effective separation of charge carriers by the potential barrier of the back contact, which causes a change in the polarity of the photocurrent.

Studies have shown that when illuminated from the side of the back electrode without a bias voltage, the area of photosensitivity of the studied SC is in the range of 400-900 nm. In the range 820-840 nm, the maximum value of $Q(\lambda)$ is observed, several times lower than when illuminated from the frontal side (Fig. 5).

This type of spectral dependence of the quantum efficiency coefficient is because when the SC is illuminated from the back side, the separation of nonequilibrium charge carriers is carried out by the SCA at the CdS-CdTe boundary, which is distant from their active generation, which causes a decrease in the photocurrent due to the increase in the negative effect of volume recombination.

With an increase in the reverse bias voltage, a significant increase in $Q(\lambda, U)$ is observed in the entire spectral range of photosensitivity. This is caused by an increase in the magnitude of the built-in electric field and the size of the space charge region, which leads to a significant reduction in losses both in the area of the separating barrier and in the reduction of recombination losses of non-equilibrium charge carriers in the volume of the base layer in the process of their diffusion to the SCA. In addition, when a negative bias is applied to the SC, the back contact SC shifts in the forward direction, which reduces its electrical resistance and thus also leads to an increase in $Q(\lambda, U)$ in the entire spectral range of photosensitivity.

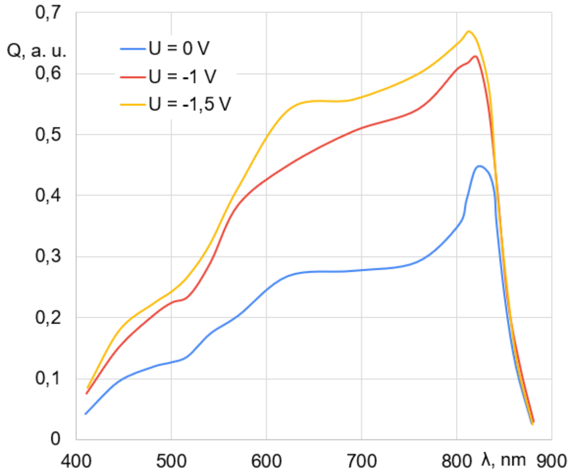

Fig. 5 – Dependency graphs of $Q(\lambda, U)$ SnO_x:F/CdS/CdTe/ITO SC when illuminated from the back side of the illumination and reverse displacement of the applied voltage

When the SC is illuminated from the rear side, an increased direct voltage bias decreases $Q(\lambda, U)$ (Fig. 6).

At $U \sim 0.5$ V, a change in the polarity of the photocurrent is observed in the entire spectral range of photosensitivity (Fig. 6). A further increase in the forward bias voltage significantly increases $Q(\lambda, U)$. The change in the polarity of the photocurrent when illuminated from the back side is caused by the above-described switching off of the SCA near the CdS-CdTe front contact and the inclusion of the p^+-CdTe-n^+-ITO back HJ with an increase in the forward bias voltage. One of the features of the formation of photocurrent, when illuminated by SC from the back side, is a decrease in the value of the forward bias, in which a change in the polarity of the photocurrent is observed to 0.5 V. This is because the region of generation of non-equilibrium charge carriers with this direction of illumination approaches the SCA of the p^+-CdTe-n^+-ITO heterojunction. As a result, the back-barrier begins to effectively separate unbalanced charge carriers at smaller SCA sizes, i.e., when applying a smaller amount of direct relative to the frontal SCA displacement.

The revealed experimentally unique dependence of the change in both the magnitude and the polarity of the quantum efficiency coefficient bifacial SC SnO_x:F/CdS/CdTe/ITO upon changing the voltage, which differs significantly for different wavelengths, was used to create a method for determining the wavelength of monochromatic irradiation of the visible range. In the specified method, at the first stage, the spectral dependences of the photocurrent were experimentally determined when illuminating the bifacial solar cell SnO_x:F/CdS/CdTe/ITO from the front and back sides. A constant direct voltage bias in the 0 – 1.2 V range with a 0.2 V step is applied to the solar cell when illuminated from the front side. When illuminating the solar cell from the back side and a similar direct voltage bias, reverse voltage biases in the 0-1.5 V range with a step of 0.5 V are applied. The obtained experimental data of photocurrent measurement were saved as a table in relative units for each wavelength. At the same time, the initial value of the photocurrent (U = 0) for each wavelength was taken as 100 %. This operation was the calibration of the installation before measurements.

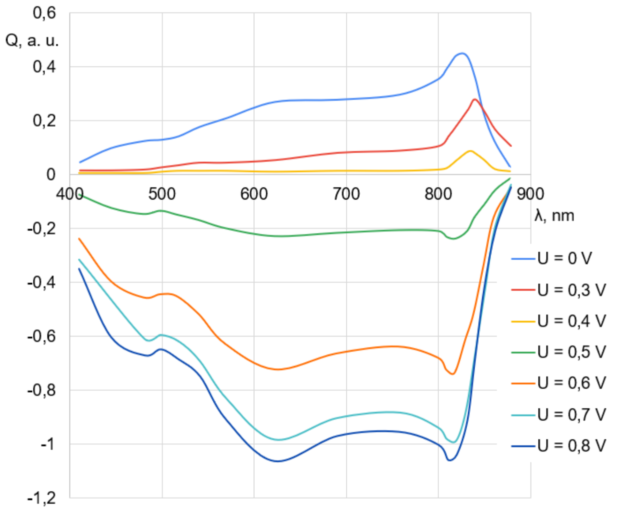

Fig. 6 – Dependency graphs of $Q(\lambda, U)$ SnO_x:F/CdS/CdTe/ITO SC when illuminated from the back side and direct displacement of the applied voltage

In the next step, the calibrated solar cell SnO_x:F/CdS/CdTe/ITO was connected to the storage oscilloscope. Then, the solar cell was illuminated by pulsed laser diode radiation from the front and back. During illumination, a constant voltage was applied to the solar cell. The voltage supply modes were the same as during SC calibration.

Using a computer program, the obtained results were compared with calibrated data. Comparison using a computer program of the obtained data with the existing database based on the minimum root mean square deviation allows for determining the wavelength of the analyzed radiation.

To measure pulse signals, it is necessary to estimate the limit frequency of the pulse. For this purpose, we investigated the dependence of the electric capacity on the applied voltage. The measurement of the dark volt-farad characteristics (VFC) of SC was carried out using a high-frequency LCR-meter HP4275A, manufactured by Hewlett Packard, by simultaneously applying to the sample a constant voltage in the range from – 2 V to + 2 V and a sinusoidal signal with a frequency of 100 kHz and an amplitude of 10 mV. According to [11], at such a signal frequency, the appearance of the VFC of CdS/CdTe-based film SCs is mainly determined by the change in the size of the space charge regions of the built-in electric fields in the device structure. The analysis shows that the maximum specific capacitance value of $16 \cdot 10^{-5}$ F/m is observed when applying a direct bias of 0.6 V. Taking into account the SC area of 0.5 cm^2 and based on the obtained maximum capacitance value, the estimate shows that the limiting frequency is 100 MHz.

4. CONCLUSIONS

A physical concept of the method for determining the wavelength of pulsed laser diode radiation developed based on the experimental measurement of the spectral dependence of the short-circuit current of bifacial thin film solar cell SnO_x:F/CdS/CdTe/ITO is proposed. The physical basis of the method is the uniqueness of the array of experimental values of the short-circuit current, which is generated during the irradiation of the SnO_x:F/CdS/CdTe/ITO SC, when it is illuminated from the front and back sides by radiation, the wavelength of which must be determined and the application of a voltage that shifts the SC in the forward direction, in the range of values of 0-1.2 V. As the forward bias voltage increases, the efficiency of the distribution of non-equilibrium charge carriers generated under the action of light by the front separating barrier CdS/CdTe decreases, and increases for the rear separating barrier CdTe/ITO. This leads to the differentiation of non-equilibrium charge carriers that are generated under the action of photons with different wavelengths due to the spectral dependence of the light absorption depth. When illuminated from the rear side, differentiation of non-equilibrium charge carriers generated by photons with different wavelengths is also achieved by applying a reverse bias in the 0-1.5 V range. In this case, the region of separation of the generated charge carriers is also shifted relative to the region of active generation.

The wavelength is determined by comparing, with the help of a computer program, the obtained values of the short-circuit current, which is generated during the irradiation of the SC, with the previously obtained numerical database of the spectral dependence of the short-circuit current of the given SC.

The main advantage of the proposed method is its compactness compared to existing analogs since instead of several thousand, it requires only one detector, which is a bilaterally sensitive SC with an area of only 0.5 cm^2. The method is also more economical because, in addition to the double-sided sensitive solar cell, the measuring kit should include only a simple storage oscilloscope on microcircuits and a stabilized direct current power supply with a voltage of up to 2 V.

REFERENCES

1. H.J. Eichler, J. Eichler, O. Lux, *Lasers: Basics, Advances and Applications* (Springer Nature Switzerland AG: 2018).
2. P.S. Kosobutskyi, *The method of envelopes in Fabry-Perot interferometry: monograph* (Lviv: Polytechnic Publishing House: 2013).
3. standa.lt/products/catalog/spectrographs_and_monochromators?item=320.
4. A.N. Tiwari, G. Khrypunov, F. Kurdzesau, D.L. Bätzner, A. Romeo, H. Zogg, *Prog. Photovolt.: Res. Appl.* **12** No 1, 33 (2004).
5. G.S. Khripunov, *Semiconductors* **40**, 113 (2006).
6. G.S. Khrypunov, G.V. Lisachuk, D.A. Kudiy, Pat. 65024, Ukraine, MPK (2006): G01J 3/50, publ. 25.11.2011, bul. № 22/2011 [In Ukrainian].
7. N.T.R.N. Kumara, A. Lim, C.M. Lim, M.I. Petra, P. Ekanayake, *Renew. Sustain. Energy Rev.* **78**, 301 (2017).
8. R.H. Bube, *Photovoltaic Materials* (USA: Imperial College Press: 1999).
9. K.M. Mitchell, A.L. Fahrenbruch, R.H. Bube, *J. Appl. Phys.* **48** No 10, 4365 (1977).
10. D.L. Batzner, G. Agostinelli, A. Romeo, H. Zogg, A.N. Tiwari, *Proceedings Materials Research Society Spring Meeting* **668**, H5.17.1 (San-Francisco: 2001).
11. G. Agostinelli, D.L. Batzner, M. Burgelman, *Proceeding 29th IEEE Photovoltaic Specialist Conference* 744 (New Orlean: 2002).

Застосування двостороннє чутливих сонячних елементів на основі телуриду кадмію для визначення довжини хвилі імпульсних лазерних діодів

Г.С. Хрипунов[1,2], А.І. Доброжан[1], М.В. Кириченко[1], Р.В. Зайцев[1], М.С. Хрипунов[1], А.В. Меріуц[1]

[1] *Національний технічний університет «Харківський політехнічний інститут», 61002 Харків, Україна*
[2] *Ecole Polytechnique Fédérale de Lausanne, CH-1015 Lausanne, Switzerland*

Запропоновано фізичну концепцію простого, економічного і компактного методу визначення довжини хвилі імпульсного випромінювання лазерного діода. У цьому методі двосторонній тонкоплівковий сонячний елемент (СЕ) SnO_x:F/CdS/CdTe/ITO використовується як датчик, який визначає довжину хвилі падаючого імпульсного випромінювання. При реалізації методу сонячний елемент SnO_x:F/CdS/CdTe/ITO освітлюється із зворотного та переднього боків імпульсним випромінюванням лазерного діода. Постійне зміщення постійної напруги в діапазоні 0-1,2 В подається на сонячний елемент при освітленні з фронтальної сторони. При освітленні сонячної батареї із тильного боку, за аналогією з прямим зміщенням напруги, застосовуються зворотні зміщення напруги в діапазоні 0-1,5 В. Довжина хвилі визначається шляхом порівняння за допомогою комп'ютерної програми отриманих значень струму короткого замикання, який виникає під час опромінення СЕ, з попередньо отриманою числовою базою даних спектральної залежності струму короткого замикання даного СЕ.

Ключові слова: Двосторонні сонячні елементи, Телурид кадмію, Довжина хвилі, Імпульсний лазерний діод, Квантовий коефіцієнт ефективності, Зміщення напруги.